Extended regions of ionized gas around active galactic nuclei

Heerde, G.M. van

Astron. Astrophys. 201, 213–222 (1988)

ASTRONOMY AND ASTROPHYSICS

Extended regions of ionized gas around active galactic nuclei *

G.M. van Heerde

Sterrewacht Leiden, Postbus 9513, 2300 RA Leiden, The Netherlands

Received January 21, accepted March 14, 1988

Summary. Narrow-band imaging of a sample of active galactic nuclei yielded a number of newly detected extra-nuclear emission line regions including a quasar, a dwarf elliptical and an X-ray-loud Seyfert. Due to the diversity of the objects exhibiting the extranuclear emission the correlation with nuclear properties as discussed by Boroson and Oke, 1984 could only partly be confirmed.

Key words: galaxies: active – galaxies: radio – galaxies: Seyfert – galaxies: nuclei of – quasars: general

1. Introduction

Extended emission line regions (EELRs after Fosbury, 1986) have been found in a number of radio galaxies with nuclear emission lines (Fosbury and Wall, 1979; Fosbury et al., 1982, 1984; Danziger et al., 1984; Smith and Robertson, 1985; Tadhunter et al., 1986) extending to tens of kiloparsecs from the nucleus. For a few radio-loud QSOs the presence of EELRs has been known for about a decade [e.g. 3C48 (Wampler et al., 1975), 4C37.43 (Stockton, 1976), 3C249.1 (Richstone and Oke, 1977)]. Recently the number of QSOs with known EELRs has increased considerably due to the successful surveys by Boroson et al. (1982), Boroson and Oke (1984) and Boroson et al. (1985) using spectroscopy and by Stockton and MacKenty (1983, 1987), who use narrow-band imaging.

An important result obtained by Boroson and coworkers which is confirmed by Stockton and MacKenty (1987) is the correlation between the presence of strong extranuclear emission lines and several *nuclear* properties: strong forbidden line emission, broad and asymmetric Balmer lines, weak or no Fe II emission and the presence of extended steep-spectrum radio lobes.

The correlation between broad, asymmetric Balmer lines and the presence of extended, steep-spectrum radio structure has been noted before by Miley and Miller (1979). The anticorrelation between Fe II strength and radio power seems to hold for radio galaxies as well (Osterbrock, 1977; Grandi and Osterbrock, 1978). Heckman et al. (1984) found a correlation between the forbidden lines and the extended radio emission for a sample of QSOs and galaxies.

The energetic jets that provide the energy input for the extended radio lobes are evidently related to the nuclear "engine"; in some cases, however, they are also related to regions of ionized gas at distances of tens to hundreds of kiloparsecs from the nucleus as has been shown convincingly by Miley et al. (1981), Heckman et al. (1982, 1984a), Phillips et al. (1984), van Breugel et al. (1984a, b; 1985a, b; 1986), and Meaburn and Pedlar (1986).

Nevertheless extended regions of ionized gas have been found in radio-quiet objects as well, e.g. the X-ray QSO MR 2251 – 178 (Bergeron et al., 1983; di Serego Alighieri et al., 1984) and a number of Seyfert galaxies (see e.g. Phillips et al., 1983a, b; De Robertis and Pogge, 1986; Wilson et al., 1986). For these objects and most of the QSOs from the Stockton and MacKenty (1987) sample a plausible explanation is usually sought in terms of interactions or mergers.

In general the presence of extranuclear emission is evidence of interaction between the active nucleus and its environment. The study of this emission can improve our understanding of both the nucleus itself and the ambient medium in the host galaxy. Examples of EELRs with particularly large linear size of luminosity will be highly valuable for understanding the basic mechanisms because those extreme cases will outline the limits of the underlying physics.

In order to contribute to the growing data base of active galaxies with EELRs and to test the correlations found with radio structure and nuclear properties a sample of active galactic nuclei (AGN) was observed using the technique of narrow-band imaging.

2. Observations

All observations were obtained using the European Space Agency (ESA) PCD in direct imaging mode at the 2.2 m telescope at the European Southern Observatory (ESO), La Silla, Chile. The PCD – Photon Counting Detector (di Serego Alighieri et al., 1985) – has been built at ESTEC as a model for the Faint Object Camera for the Space Telescope and has been available as a common user instrument at ESO in 1985 and 1986. The data reduction procedure is described by van Heerde (1988).

Of major importance here is a non-linearity of the PCD causing an uncertainty of about 50% in the absolute flux calibration. A direct consequence is the large uncertainty in the subtraction of a continuum image: if the extranuclear emission follows the distribution of the starlight no unambiguous result can be obtained. Only where the line emission is much more prominent

* Based on observations collected at the European Southern Observatory, La Silla, Chile

than the continuum emission (regions characterized by a very large equivalent width) a positive detection can be made.

To improve the consistency of line and continuum images the presence of field stars could be used for an additional internal calibration (under the assumption that the average spectrum of the stars is identical to that of the continuum to be subtracted over the wavelength range covered by the filters.

A well-known limitation of all photon counters is the saturation of bright objects due to the finite frame rate inhibiting detection of more than a few photons per point source per frame (the kind of saturation that results is not accumulative as in CCDs but instantaneous; therefore it does not set limits to the total integration time but to the surface brightness of the object).

The sample was selected from the catalogue of quasars and active nuclei (Véron-Cetty and Véron, 1985, hereafter VV) containing all objects with known radio flux for which $z < 0.4$ (the range for which narrow-band filters were available for [O II] λ3727 and [O III] λ5007), $V > 15.5$ (to avoid saturation of the nucleus) and $\delta < 20°$. This sample contains a total of 89 candidate objects of which a further selection was made according to observable hour angle and availability of a matching filter. A final sample of 47 objects was thus obtained of which 15 objects were observed during an observing run in January, 1986 using narrow-band interference filters centred on either [O III] λ5007 or [O II] λ3727.

Earlier, in February and April 1985, 8 objects were observed during preliminary runs at ESO with the purpose of obtaining representative material. These objects were partly selected on the basis of published results and will be discussed along with the objects from the main sample in the next section.

A standard PCD image contains 512 × 512 pixels each 0″.293 in size. Typical exposure times are 30 min.

The observations are summarized in Table 1. For some objects which were judged unresolved in the line filter no corresponding continuum image was obtained. Table 1 contains the following columns:

Col. 1: Object designation; an asterisk indicates that the object was part of the preliminary sample
Col. 2: Object name
Col. 3: Object type (Sy: Seyfert galaxy; NLRG: Narrow Line Radio Galaxy; BLRG: Broad Line Radio Galaxy; QSR: radio-loud QSO)
Col. 4: Redshift (from VV)
Col. 5: Apparent visual magnitude V (from VV)
Col. 6: radio flux at 6 cm (from VV)
Col. 7: Central wavelength/bandwidth (FWHM), in Å, for the filter
Col. 8: Exposure time in seconds
Col. 9: Type of observation: line ([O II] λ3727 or [O III] λ5007) or continuum or BLUE (broad band low pass filter)

3. Results

The results are presented in Table 2 which contains the following columns:

Col. 1: Object name
Col. 2: Type of observation: line ([O II] λ3727 or [O III] λ5007) or continuum or BLUE (broad band low pass filter)
Col. 3: Observed flux density within the filter bandwidth in milliJansky (1 mJy = 10^{-26} erg/cm^2/s/Hz)
Col. 4: Observed AB magnitude per unit frequency within the filter (conversion from mJy to AB mag from Stone and Baldwin, 1983)
Col. 5: Background noise level (1 σ) in mag/arcsec^2; indication of the lowest detectable surface brightness
Col. 6: Continuum subtracted pure line flux density (average over filter)
Col. 7: Integrated line flux
Col. 8: Total emission line luminosity (using $H_0 = 50$ km s^{-1}/Mpc and $q_0 = 0.5$ which is used throughout this paper)
Col. 9: Comments

Because of the uncertainty in the absolute calibration which causes an uncertainty in the resulting continuum subtracted line image, in all cases where we believe the extended emission to be real the observed line and continuum images are given as well.

Comparing published V and B magnitudes with the observed continuum magnitudes (for the 12 objects for which both are available) led to the conclusion that no serious systematic errors are present. For 8 objects both magnitudes agree within 0.5 mag.

One object appeared to have faded more than three magnitudes (4C12.50) and will be described in more detail below. Three objects were 1.5 to 2 mag brighter than the published value (PKS 0231+022, 1E1225+089 and 3C323.1). These objects are most likely variable (for 3C323.1 this result is consistent with the increase in brightness observed by Hunter and Lü, 1969).

Because of calibration uncertainties small relative differences in the line and continuum fluxes are considered doubtful.

Although no continuum images are available it can be deduced that two objects (PHL 1093 and PKS 1151−348) have faded 0.5 to 1 mag (and more if the line emission is strong) and that 4C09.31 has very strong [O II] emission (~40 nm equivalent width) unless variability is dominant.

Some of the objects from the preliminary sample did not yield the expected result. 3C206 had been studied in detail by Wyckoff et al. (1980) who presented a deep exposure in which the quasar was clearly resolved and centered in a compact cluster of galaxies. A spectrum of the envelope shows narrow Hβ, [O II] and [O III] emission. Neither the surrounding galaxies nor any fuzz surrounding the quasar is visible in the narrow-band images centered on [O II] and nearby continuum. Detailed profile comparisons between line and continuum images have not been made, however, because the flux-dependent non-linearity of the PCD (van Heerde, 1988) results in profile differences depending on brightness.

1E1225+089 was included in the preliminary sample inspired by the succesful imaging of the X-ray-loud QSO MR2251−178 by di Serego Alighieri et al. (1984). Another null result, Mkn 841, of which a nebulosity spectrum has been published by Boroson et all. (1982) has been discussed elsewhere (van Heerde, 1986).

4. Discussion of individual objects

X0459+034

This low-redshift compact X-ray luminous Seyfert 1.5 galaxy was found to be a strong [O III] emitter with significant extended emission surrounding the nucleus. The line images centered on [O III] (Fig. 1) and [O II] (Fig. 2) both show irregular outer contours which are not present in the continuum image (Fig. 3) revealing a smooth galaxy with a maximum extent of ~13 kpc (to a surface brightness of 24 mag/arcsec^2). Note the faintness of the two objects to the North West in the [O II] image indicating their very red color.

The pure [O III] image (Fig. 4) shows a bright arm extending from the South end of the galaxy toward the West. This arm is also

Table 1

Designation	Name	Type	z	V (mag)	S_6 (mJy)	Filter ($\lambda_0/\Delta\lambda$)	T (s)	Obs.
0137+012	PHL 1093	QSR	0.258	17.07	830	4705/96	1800	[O II]
0231+022	PKS	QSR	0.332	18.	59	5009/103	1800	[O II]
						4705/96	1800	Cont
0336−355	PKS	NLRG	0.113	19.	1400 [a]	4118/160	3600	[O II]
						4510/103	1800	Cont
0410+110	3C109	BLRG	0.306	18.01	1640	4867/34	1800	[O II]
0449−184	1E	QSO	0.338	18.5	1.1	5009/103	1800	[O II]
0450−182	1E	QSO	0.059	17.8	2.6	5306/36	1800	[O III]
0459+034	X	Sy 1.5	0.016	15.	5.2	5100/103	1800	[O III]
						4705/96	1800	Cont
						3796/32	3600	[O II]
0511+008	3C135	BLRG	0.127	17.00	1080	4183/55	1800	[O II]
0723−008	OI-039	BLRG	0.127	18.	2250	4183/55	1800	[O II]
						4046/52	1800	Cont
0837−120*	3C206	QSR	0.200	15.8	760	4474/36	2800	[O II]
						4330/32	1600	Cont
0846+100	4C09.31	QSR	0.366	19.20	500 [a]	5100/103	1800	[O II]
0949−013*	Mkn 1239	Sy 1.5	0.019	14.39	—	5100/103	1800	[O III]
						4705/96	1800	Cont
1007−426*	F 427	Sy 2	0.033	—	—	5191/39	1800	[O III]
						5060/20	3600	Cont
1032−271*	TOL	QSO	0.06	18.1	—	5306/36	3600	[O III]
						5009/103	1800	Cont
1151−348	PKS	QSR	0.258	17.84	2730	4705/96	1800	[O II]
1220+051*	TOL	Sy 2	0.018	17.13	—	5100/103	1800	[O III]
						4705/96	1800	Cont
						$\leqq$4600	3600	Blue
1225+089*	1E	QSO	0.085	16.64	—	5448/40	3000	[O III]
						5100/103	1200	Cont
1300+166	Mkn 783	Sy 1	0.068	15.55	3	5335/39	1500	[O III]
1345+125	4C12.50	NLRG	0.121	17.0	2920	4183/55	1800	[O II]
						4046/52	950	Cont
1350−381	TOL	Sy 2	0.060	15	89	5306/36	1460	[O III]
1417−192	PKS	BLRG	0.119	16.66	71	4183/55	1800	[O II]
1501+106*	Mkn 841	Sy 1	0.036	14.27	—	5191/39	1800	[O III]
						5263/38	1800	Cont
1545+210*	3C323.1	QSR	0.264	16.69	920	4705/96	5400	[O II]
						4510/103	1200	Cont

[a] Radioflux at 11 cm

visible in the pure [O II] image (Fig. 5) but the counter arm is more conspicuous in the [O II] image extending from the NE side of the galaxy toward the SE. A number of condensations can be distinguished in both arms.

Present in both pure line images is a broad resolved feature extending from the nucleus toward the NW. A fainter feature on the opposite side is also visible.

Comparison of the total fluxes with the values obtained by Ghigo et al. (1982) is not possible since they do not give the slit size used for their nuclear spectra.

MKN 1239

Indications for interaction can be found in the [O III] image of the bright peculiar type 1.5 Seyfert galaxy Mkn 1239, known for its IR

Table 2

Name	Obs.	Flux (mJy)	Flux (AB)	Backgr. (mag/″^{2})	f (mJy)	F (erg/cm^2/s)	log L (erg/s)	Comments
PHL 1093	[O II]	240	18.0	22.8				
PKS 0231+022	[O II]	750	16.7	23.3	~ 0			
	Cont	830	16.6	23.6				
PKS 0336−355	[O II]	110	18.9	24.0	~ 0			
	Cont	140	18.5	23.7				
3C109	[O II]	330	17.6	22.1				
1E 0449−184	[O II]	250	17.9	23.9				
1E 0450−182	[O III]	780	16.7	23.2				
X 0459+034 [a]	[O III]	10800	13.8	23.6	7200 (1700)	$9.1\ 10^{-13}$ ($2.1\ 10^{-13}$)	42.0 (41.4)	P.A. = 315°
	Cont	3600 [b]	15.0	24.4				
	[O II]	6200	14.4	23.5	3900 (900)	$2.5\ 10^{-13}$ ($5.8\ 10^{-14}$)	41.5 (40.8)	P.A. = 315°
	Cont	2300 [c]	15.5	24.8				
3C135	[O II]	240	18.0	23.8				
OI−039	[O II]	260	17.8	23.9	~ 0			
	Cont	270	17.8	23.9				
3C206	[O II]	1400	16.0	23.9	200	$1.2\ 10^{-14}$	42.4	Unresolved
	Cont	1200	16.2	23.9				
4C09.31	[O II]	330	17.6	24.0				
Mkn 1239	[O III]	8700	14.1	23.9	2800	$3.5\ 10^{-13}$	41.7	Slightly res.
	Cont	5900	14.5	23.9				
Assoc Gal	[O III]	3050	15.2	23.9	850	$1.1\ 10^{-13}$	41.2	at 75″ in
	Cont	2200	15.5	23.9				P.A. = 192°
F 427	[O III]	3550	15.0	23.7	1650	$1.0\ 10^{-13}$	41.7	Slightly res.
	Cont	1900	15.7	24.1				
TOL 1032−271	[O III]	1610	15.9	24.1	1440	$6.0\ 10^{-14}$	42.0	Unresolved
	Cont	170	18.3	24.1				
PKS 1151−348	[O II]	80	19.1	24.3				
TOL 1220+051	[O III]	3200	15.1	23.9	2960	$4.0\ 10^{-13}$	41.7	Unresolved
	Cont	240	18.0	24.3				
	Blue	310	17.7	26.4				
Condensation	[O III]	35	20.0	23.9	30	$4.2\ 10^{-15}$	39.8	at 6″ in
	Cont	5	22.2	24.3				P.A. = 84°
	Blue	8	21.6	26.4				
1E 1225+089	[O III]	4910	14.7	23.9	220	$1.1\ 10^{-14}$	41.5	Unresolved
	Cont	4690	14.7	23.7				
Mkn 783	[O III]	7860	14.2	22.3				
4C12.50	[O II]	160	18.4	23.8	130	$1.3\ 10^{-14}$	41.9	Unresolved
	Cont	30 [d]	20.2	23.0				
TOL 1350−381	[O III]	1300	16.1	21.4				
PKS 1417−192	[O II]	920	16.5	23.8				
Mkn 841	[O III]	15900	13.4	24.3	7600	$3.7\ 10^{-13}$	42.3	Unresolved
	Cont	8300	14.1	24.1				
3C323.1	[O II]	2900 [e]	15.2	24.2	0 [f]			
	Cont	2900 [f]	15.2	23.4				
Companion	[O II]	50	19.7	24.2	30	$4.0\ 10^{-15}$	42.1	At 11″ in
	Cont	20	20.7	23.4				P.A. = 280°

[a] Between brackets are given the estimated values for the extranuclear emission only; [b] [O III] image multiplied by 0.77 before continuum subtraction; [c] [O II] associated continuum multiplied by 0.64 before subtraction; [d] Continuum image multiplied by 1.6 before subtraction; [e] Three line images internally "matched" using factors 1.15 and 1.22 for second and third image, respectively; [f] Internal calibration on one star would make the continuum flux larger than the observed line flux. To get a conservative lower limit to the [O II] flux of the blob the continuum image was multiplied by 1.10 to make the continuum flux of the QSO equal to the line flux

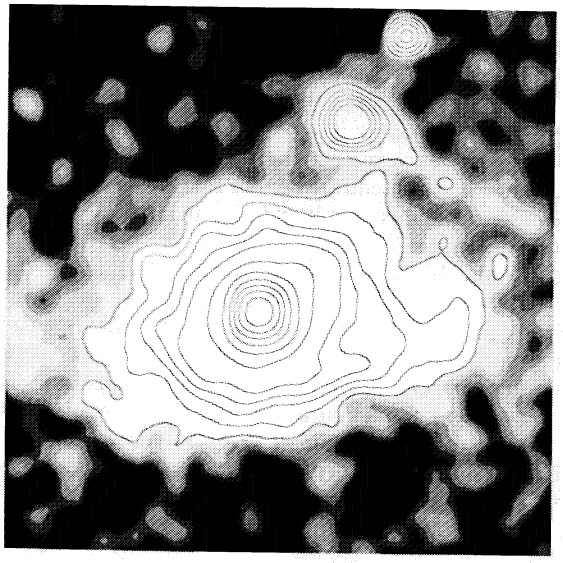

Fig. 1. X 0459+034 line image ([O III]), smoothed to 2″ FWHM to enhance low surface brightness structures. Field measures 45″ on a side. North is to the top, East to the left. Contour levels at 0.2, 0.33, 0.5, 0.75, 1, 2, 4, 8, 16, 32, and 64 μJy/pix (1 μJy/pix corresponds to $11.6\ 10^{-29}$ ergs/cm^2/s/Hz/arcsec^2 or 21.2 mag/arcsec^2). Gray levels emphasäe the noise; Black is zero flux and 8 shades of gray are roughly logarithmically spaced between zero and the lowest contour level

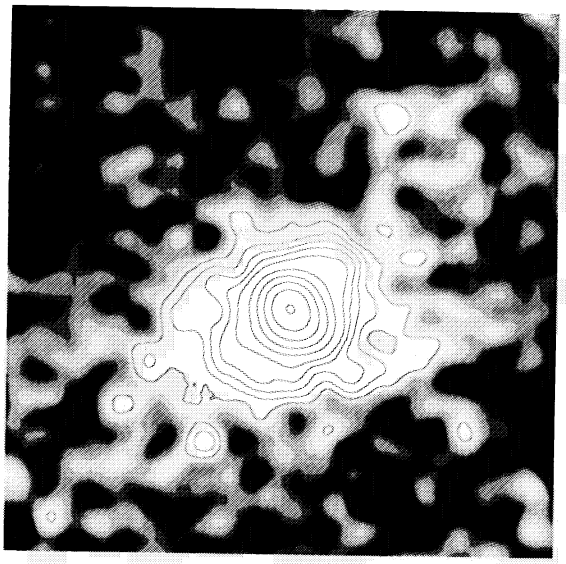

Fig. 2. X 0459+034 line image ([O II]). Highest contour level: 32 μJy/pix, see further Fig. 1

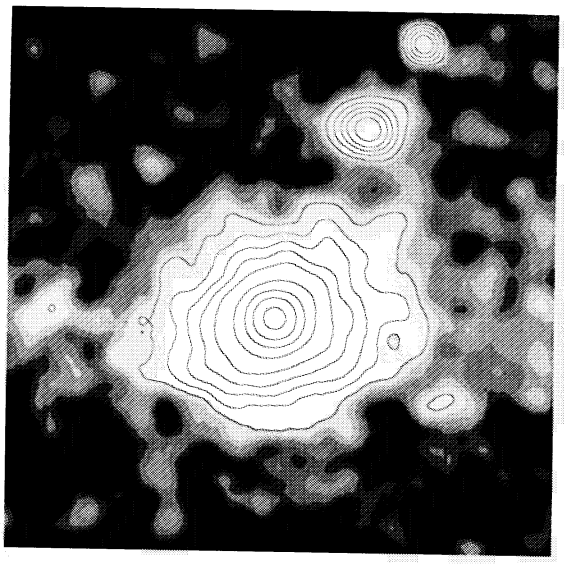

Fig. 3. X 0459+034 continuum image. Highest contour level: 16 μJy/pix, see further Fig. 1

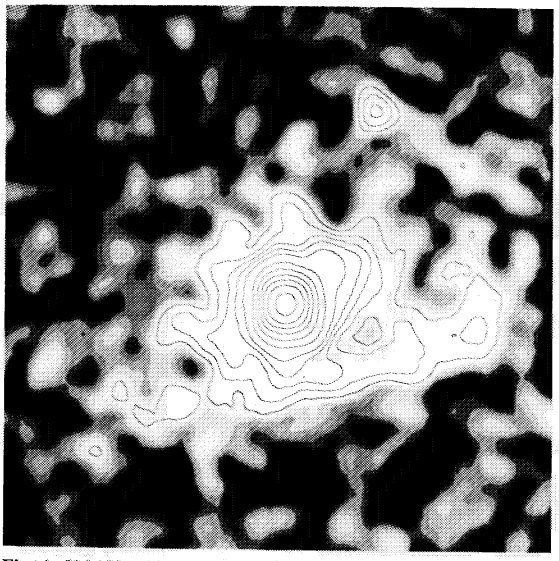

Fig. 4. X 0459+034 pure [O III] image. Highest contour level: 64 μJy/pix, see further Fig. 1

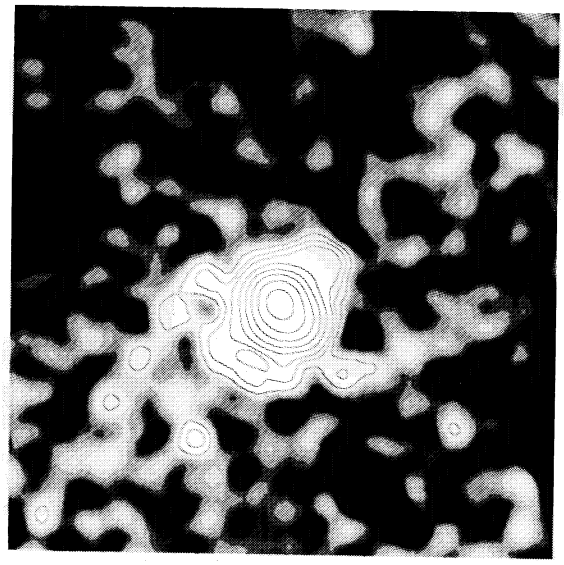

Fig. 5. X 0459+034 pure [O II] image. Highest contour level: 16 μJy/pix, see further Fig. 1

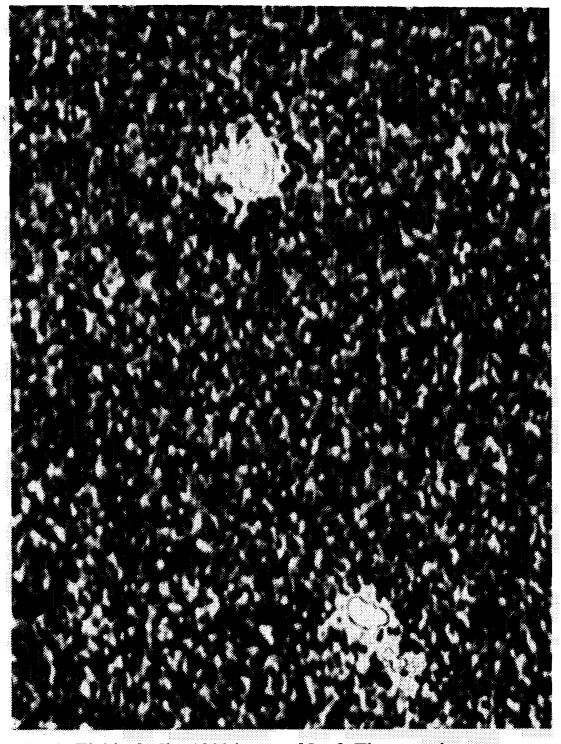

Fig. 6. Field of Mkn 1239 in pure [O III]. The area shown measures 1'.5 × 2'. For details see Figs. 9 and 12

excess and unusually broad [O III] lines, ~1300 km s^{-1} (Rafanelli and Bonoli, 1984). There is no evidence for extended emission around this slightly resolved galaxy but a companion galaxy at a projected distance of 40 kpc appears to be highly excited (Fig. 6). Probably the galaxy is undergoing a burst of star formation which could be triggered by a recent encounter with the nearby Seyfert galaxy. The emission is concentrated on the side facing the Seyfert where 75% of the [O III] flux is emitted (more than 10^{41} erg s^{-1} in an region of roughly $4 \times 2^1/_2$ kpc).

Figures 7–9 and 10–12 show the observed [O III] image, the emission-line free continuum and the pure [O III] image of Mkn 1239 and the companion galaxy, respectively. The irregular shape of the nuclear [O III] image (Fig. 9) is a result of slight distortions in the point spread function of the line image (Fig. 7) being enhanced after subtraction of the continuum image. The continuum image of the companion (Fig. 11) shows a rather smooth distribution without a clear nucleus. Superposed are several large complexes of H II regions (Fig. 12).

TOL 1032−271

This low-luminosity AGN resides in a compact galaxy (largest size less than ~10 kpc) with very strong [O III] emission (W_{eq} ~ 35 nm) from the nucleus which appears double on POSS plates, a possible indication of interaction between two galaxies. It was included for

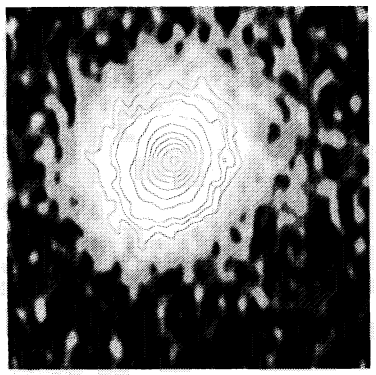

Fig. 7. Mkn 1239 line image ([O III]). The field measures 30″ on a side. Contour levels are at 0.5, 0.75, 1, 2, 4, 8, 16, 32, 64, and 128 μJy/pix. Gray levels as in Fig. 1

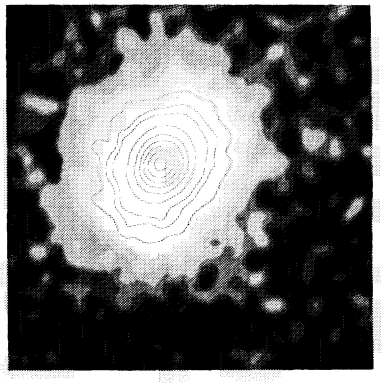

Fig. 8. Mkn 1239 continuum image. Highest contour level: 64 μJy/pix, see further Fig. 7

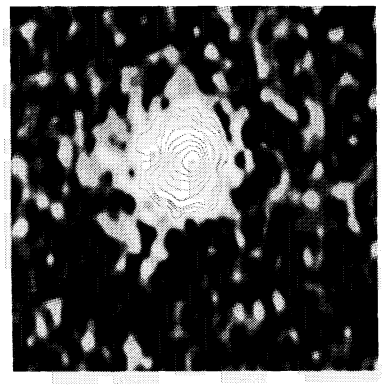

Fig. 9. Mkn 1239 pure [O III] image. Highest contour level: 64 μJy/pix, see further Fig. 7

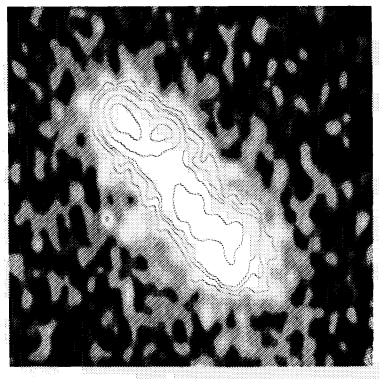

Fig. 10. Companion galaxy of Mkn 1239, line image ([O III]). Highest contour level: 4 μJy/pix, see further Fig. 7

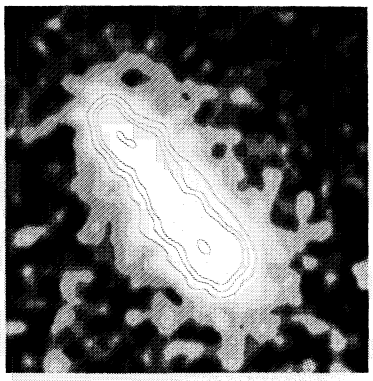

Fig. 11. Companion galaxy of Mkn 1239, continuum image. Highest contour level: 2 μJy/pix, see further Fig. 7

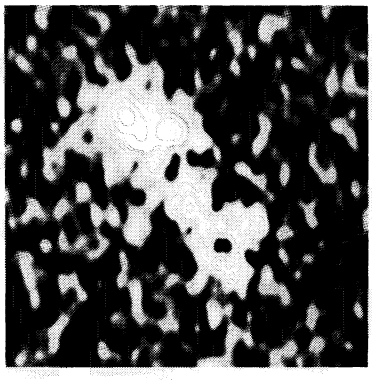

Fig. 12. Companion galaxy of Mkn 1239, pure [O III] image, Highest contour level: 4 μJy/pix, see further Fig. 7

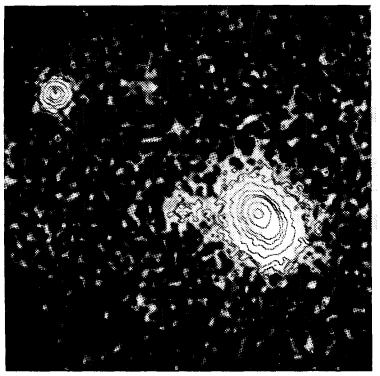

Fig. 13. FOL 1220+051 broad-band blue image. Field measures 30″ on a side. Contour levels at 0.08, 0.12, 0.25, 0.5, 1, 2, and 4 μJy/pix. Gray levels see Fig. 1

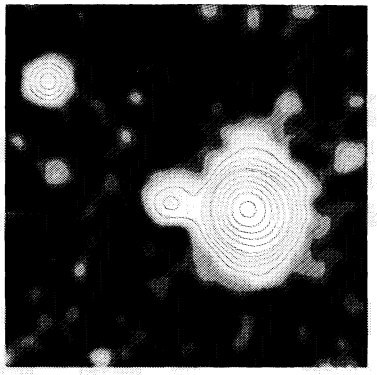

Fig. 14. TOL 1220+051 line image ([O III]) smoothed to 2″ FWHM to enhance low surface brightness structures. Field measures 30″ on a side. Contour levels at 0.2, 0.33, 0.5, 0.75, 1, 2, 4, 8, 16, and 32 μJy/pix. Gray levels see Fig. 1

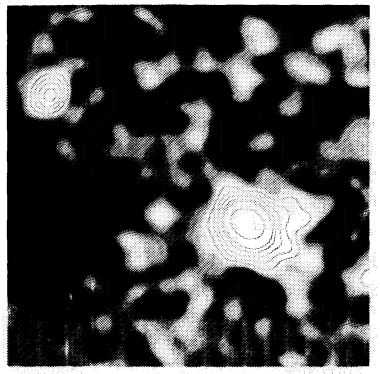

Fig. 15. TOL 1220+051 continuum image. Highest contour level: 2 μJy/pix, see further Fig. 14

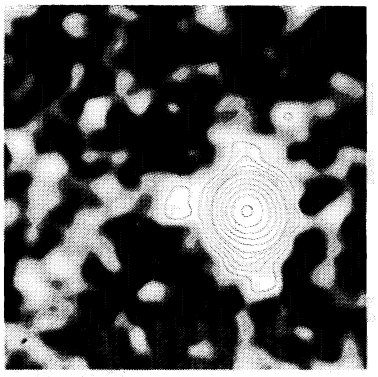

Fig. 16. TOL 1220+051 pure [O III] image. Highest contour level: 32 μJy/pix, see further Fig. 14

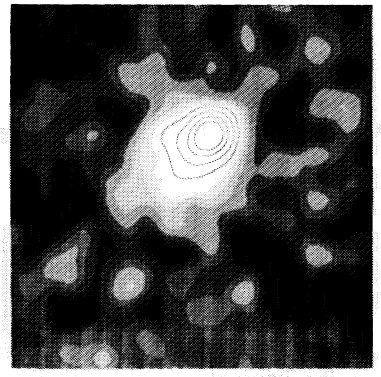

Fig. 17. 4C12.50 line image ([O II]) smoothed to 2″ FWHM to enhance low surface brightness structures. Field measures 30″ on a side. Contour levels at 0.33, 0.5, 0.75, and 1 μJy/pix. Gray levels as Fig. 1

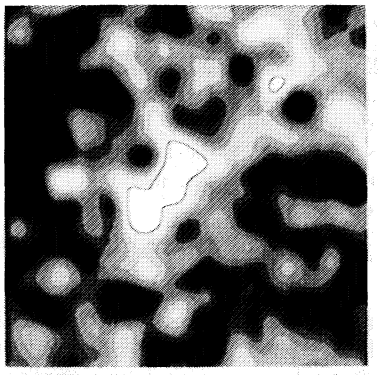

Fig. 18. 4C12.50 continuum image. Contour level at 0.33 μJy/pix, see further Fig. 17

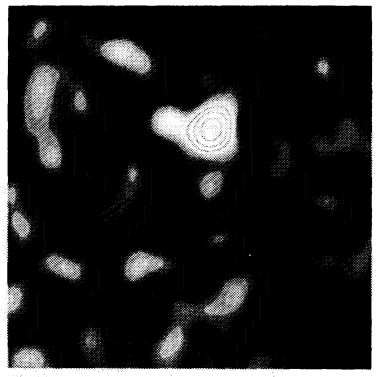

Fig. 19. 4C12.50 pure [O II] image. Highest contour level: 0.75 μJy/pix, see further Fig. 17

this reason as in a similar case, 0351+026 the strongest extra-nuclear [O III] emission was found in a bridge connecting the nuclei of both galaxies (Bothun et al., 1982).

But no bridge of emission was found. Subtraction of the continuum removes the companion galaxy completely. At a separation of 4.″2 (corresponding to 6.8 kpc) the probability of a physical association is very high (see e.g. Heckman et al., 1984b). Note the similarity with the "QSO-galaxy binary" presented by Gilmore, 1984 in which the companion galaxy emits only weak [O II] λ3727 emission although the QSO is capable of ionizing all the gas in the galaxy (Filippenko, 1985).

TOL 1220+051

Although originally classified as a low-redshift QSO by Bohuski, Fairall and Weedman, 1978 because of its star-like appearance and Seyfert 1 colors, TOL 1220+051 is a dwarf Seyfert 2 galaxy. It is clearly resolved on a broad-band exposure (a low-pass filter cutting off at 460 nm was used). In Fig. 13 the "QSO" is the nucleus of a small galaxy (the major axis is 8″ or 4 kpc) with

smooth elliptical contours and an axial ratio of ~0.75. Remarkably the outer contours are not centered on the nucleus but on a point displaced by ~0″.8 along the major axis.

To the East of the nucleus a faint bridge of emission connects the galaxy to a low surface brightness condensation. This condensation at a distance of 6″ or 3 kpc from the nucleus is clearly present in the line image (centered on [O III], Fig. 14) and possibly also in the continuum image but much fainter (Fig. 15).

The condensation is therefore mostly composed of emission line gas. The bridge of emission consists purely of ionized gas as it is definitely absent in the continuum image. The enhancement in the bridge in the broad-band exposure could be due to [O II] and/or [Ne III] emission. Long-slit spectroscopy is needed to clarify this situation.

The small size and the low luminosity make TOL 1220+051 even smaller than the dwarf Seyfert discovered by Kunth, Sargent and Bothun, 1987. After the discovery of low-level activity in "normal" galaxies (Keel, 1983a, b; Filippenko and Sargent, 1985) the discovery of active nuclei in dwarf galaxies show that nuclear activity can be a property of galaxies on all scales.

4C12.50

The compact radio source 4C12.50 (PKS 1345+12) is unusual among narrow-line radio galaxies because of its very broad forbidden lines: the low-ionization lines have a FWHM of ~1200 km s^{-1}; the high-ionization lines are even broader and have the same width as the Balmer lines: FWHM ~1600 km s^{-1} (Grandi, 1977).

A recent broad-band R-image presented by Gilmore and Shaw, 1986 reveal a large envelope surrounding a distorted giant elliptical with two nuclei. The eastern nucleus, coincident with the radio source is very red; the bluer western nucleus is the source of the line emission. A scenario involving a merger between an elliptical and a spiral was proposed to explain the unusual properties of this galaxy.

The narrow-band images centered on [O II] show a nucleus with faint extensions toward the South East and the East (Fig. 17). The (blue) continuum is very faint (Fig. 18). The AB magnitude near 400 nm is estimated at 20.2 mag making the galaxy over three magnitudes fainter in the blue than the visual magnitude estimated by Clarke et al. (1966). The very red color is confirmed by Gilmore and Shaw who note the absence of any blue continuum in their spectrum of the bluer western nucleus.

After subtraction of the continuum the SW extension disappears (see Fig. 19). In spite of the asymmetric location of the fuzz with respect to the emission peak (i.e. the western nucleus in Gilmore and Shaw) there is no trace of any extranuclear emission. (Considering the poor signal-to-noise of the extension and the rather noisy continuum image the loss of a possibly real extension is not unlikely). The condensation to the East of the nucleus is an artifact caused by subtraction of the noisy continuum. Gilmore and Shaw, also, do not find any spatially resolved line emission.

3C323.1

Another example where an active nucleus is capable of ionizing gas outside the main body of the parent galaxy is the quasar 3C323.1. The detection of strong extranuclear [O III] emission by Boroson and Oke (1984) was reason to include this object in the preliminary sample. Due to the poor sensitivity of the PCD redward of 550 nm 3C323.1 was observed in the light of [O II] λ3727 although very little was known of the blue spectrum.

In the long exposure (90 min through a 9.6 nm wide filter centered on [O II] λ3727, Fig. 20) there is no sign of the compact object 2″.7 to the NW of the QSO described by Stockton, 1982. It must be a very red object as the red magnitude is given by Stockton to be 20.0 mag. Because the [O III] emission reported by Stockton is due to an envelope of ionized gas surrounding the QSO (Stockton and MacKenty, 1987) and not to the compact object itself it is likely to be a compact red galaxy similar to the object near Mkn 205 (Stockton et al., 1979).

But an inspection of our line and continuum images reveals [O II] emission from another compact object in the field: the stellar object 11″ to the West of the QSO is about one magnitude brighter in the line image (Fig. 20) than in the corresponding continuum image (Fig. 21). It could be a member of the rich cluster found by Oemler et al. (1972) at the same redshift as the QSO. At a projected distance of 60 kpc the quasar could easily ionize the gas in this presumed companion galaxy (Filippenko, 1985).

The reality of this excess (in view if the calibration uncertainty) could be confirmed by taking a conservative approach in the determination of the pure line flux: I have assumed that there is no *nuclear* [O II] emission from 3C323.1 thus obtaining a lower limit to the [O II] flux of the stellar object. The residual [O II] emission peak of the QSO (see Fig. 22) is due to profile difference between line and continuum images (the accompanying negative dip is not shown but the total flux is equal to zero).

A good spectrum of the object will be necessary to determine its nature and to ascertain its relation to 3C323.1 (the possibility that it is a background QSO with one of its emission lines redshifted into the observed wavelength band cannot be excluded at the moment).

The radio emission of 3C323.1 appears to be unrelated to either object, 3C323.1 being a 1′.5 wide double-lobed radio source with its radio axis running NW–SW (Pooley and Henbest, 1974).

5. Conclusions

Narrow-band observations of a sample of active galactic nuclei led to the detection of a small but very diverse subsample of objects exhibiting some kind of extranuclear line emission. The low "succes rate" (1 out of 15 or 7%) compared to other surveys (e.g. Boroson et al., 1985; Stockton and MacKenty, 1987; Tadhunter as reported by Fosbury, 1986) is probably partly due to the poor detection efficiency of the PCD (van Heerde, 1988) and partly to the choice of objects. As the preliminary sample was heavily biased toward "interesting" objects the higher succes rate of 3 out of 7 (43%) is not surprising.

The four objects with definite extranuclear emission include a radio-loud steep-spectrum QSO with extended radio emission, a dwarf Seyfert 2 galaxy, an X-ray emitting radio-weak intermediate Seyfert galaxy and a companion galaxy of another intermediate Seyfert galaxy. Because of the small number of objects involved and their diversity no conclusive statements can be made about the correlations found by Boroson and Oke (1984). Strong nuclear narrow-line emission, however, is present in all cases, confirming this apparently necessary but not sufficient condition.

Considering the morphology of the extranuclear emission two main types can be distinguished: condensations or detached emission line regions (3C323.1 and TOL 1220+051) and arms or tails emanating from the nucleus (X 0459+034 and possibly 4C12.50); the companion of Mkn 1239 is not considered a proper extranuclear emission line region in this respect as it is now a

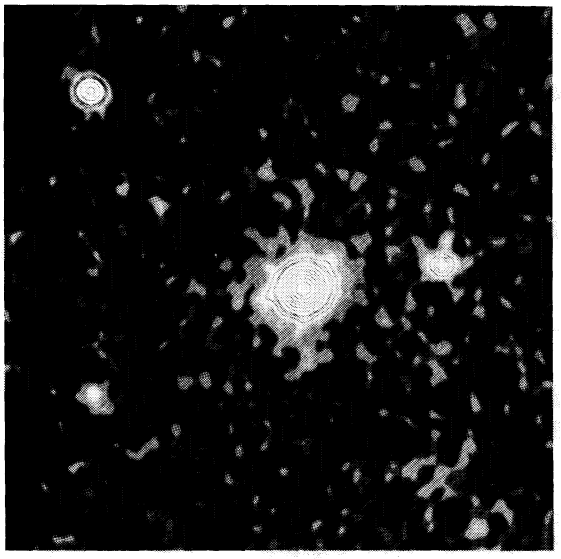

Fig. 20. 3C323.1 line image ([O II]). Field measures 45″ on a side. Highest contour level: 64 μJy/pix, see further Fig. 1

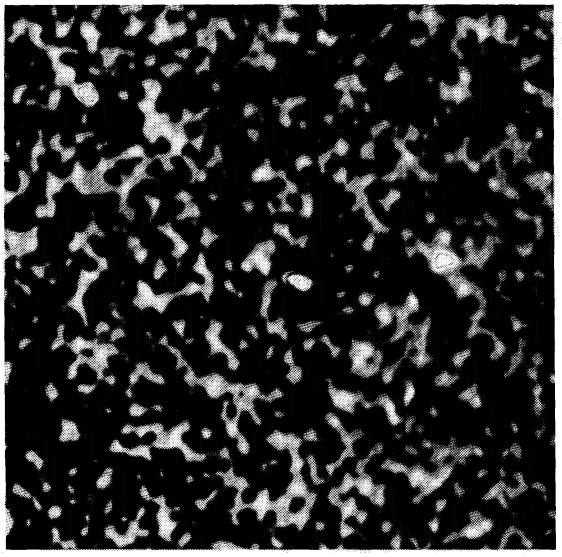

Fig. 22. 3C323.1 pure [O II] image. Highest contour: 8 μJy/pix. Emission peak at the location of the QSO is due to mismatch between line and continuum profiles. See further Fig. 20

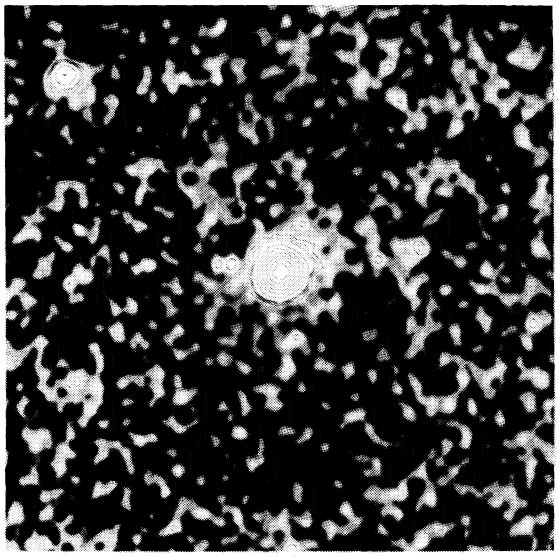

Fig. 21. 3C323.1 continuum image, as Fig. 20

completely separate galaxy possibly excited by Mkn 1239 during an encounter in the past.

To determine the nature of the emission line regions and to understand the properties of the two proposed morphological types long-slit spectroscopy of some of the objects is being undertaken.

Acknowledgements. I would like to express my gratitude toward Wim Brokaar and Loek Zuiderduin for providing all photographs and to Harry van der Laan, Rudolf le Poole and Jan Lub for useful discussions. I am indebted to Sperello di Serego Alighieri for a careful reading of the manuscript and many useful suggestions.

ESTEC is acknowledged for financial support during this project.

References

Bohuski, T.F., Fairall, A.P., Weedman, D.W.: 1978, *Astrophys. J.* **221**, 776

Bergeron, J., Boksenberg, A., Dennefeld, M., Tarenghi, M.: 1983, *Monthly Notices Roy. Astron. Soc.* **202**, 125

Boroson, T.A., Oke, J.B.: 1984, *Astrophys. J.* **281**, 535

Boroson, T.A., Oke, J.B., Green, R.F.: 1982, *Astrophys. J.* **263**, 32

Boroson, T.A., Persson, S.E., Oke, J.B.: 1985, *Astrophys. J.* **293**, 120

Bothun, G.D., Mould, J., Heckman, T.M., Balick, B., Schommer, R.A., Kristian, J.: 1982, *Astron. J.* **87**, 1621

Clarke, M.E., Bolton, J.G., Shimmins, A.J.: 1966, *Australian J. Phys.* **19**, 375

Danziger, I.J., Fosbury, R.A.E., Goss, W.M., Bland, J., Boksenberg, A.: 1984, *Monthly Notices Roy. Astron. Soc.* **208**, 589

De Robertis, M.M., Pogge, R.W.: 1986, *Astron. J.* **91**, 1026

di Serego Alighieri, S., Perryman, M.A.C., Macchetto, F.: 1984, *Astrophys. J.* **285**, 567

di Serego Alighieri, S., Perryman, M.A.C., Macchetto, F.: 1985, *Astron. Astrophys.* **149**, 179

Filippenko, A.V.: 1985, *Astron. J.* **90**, 1172

Filippenko, A.V., Sargent, W.L.W.: 1985, *Astrophys. J. Suppl. Ser.* **57**, 503

Fosbury, R.A.E.: 1986, in *Structure and Evolution of Active Galactic Nuclei*, Trieste, April 10–13, 1985, eds. G. Guiricin et al., p. 297

Fosbury, R.A.E., Wall, J.V.: 1979, *Monthly Notices Roy. Astron. Soc.* **189**, 79

Fosbury, R.A.E., Boksenberg, A., Snijders, M.A.J., Danziger, I.J., Disney, M.J., Goss, W.M., Penston, M.V., Wamsteker, W., Wellington, K.J., Wilson, A.S.: 1982, *Monthly Notices Roy. Astron. Soc.* **201**, 991

Fosbury, R.A.E., Tadhunter, C.N., Bland, J., Danziger, I.J.: 1984, *Monthly Notices Roy. Astron. Soc.* **208**, 955

Ghigo, F.D., Wyckoff, S., Wardle, J.F.C., Cohen, N.L.: 1982, *Astron. J.* **87**, 1438

Gilmore, G.: 1984, *Monthly Notices Roy. Astron. Soc.* **211**, 25p
Gilmore, G., Shaw, M.A.: 1986, *Nature* **321**, 750
Grandi, S.A.: 1977, *Astrophys. J.* **215**, 446
Grandi, S.A., Osterbrock, D.E.: 1978, *Astrophys. J.* **220**, 783
Heckman, T.M., Bothun, G.D., Balick, B., Smith, E.P.: 1984, *Astron. J.* **89**, 958
Heckman, T.M., Miley, G.K., Balick, B., van Breugel, W.J.M., Butcher, H.R.: 1982, *Astrophys. J.* **262**, 529
Heckman, T.M., Miley, G.K., Green, R.F.: 1984, *Astrophys. J.* **281**, 525
Heckman, T.M., van Breugel, W.J.M., Miley, G.K.: 1984, *Astrophys. J.* **286**, 509
Hunter, J., Lü, P.: 1969, *Nature* **223**, 1045
Keel, W.C.: 1983a, *Astrophys. J.* **268**, 632
Keel, W.C.: 1983b, *Astrophys. J.* **269**, 466
Kunth, D., Sargent, W.L.W., Bothun, G.D.: 1987, *Astron. J.* **93**, 29
Meaburn, J., Pedlar, A.: 1986, *Astron. Astrophys.* **159**, 336
Miley, G.K., Heckman, T.M., Butcher, H.R., van Breugel, W.J.M.: 1981, *Astrophys. J. Letters* **247**, L5
Miley, G.K., Miller, J.S.: 1979, *Astrophys. J. Letters* **228**, L55
Oemler, A., Gunn, J.E., Oke, J.B.: 1972, *Astrophys. J. Letters* **176**, L47
Osterbrock, D.E.: 1977, *Astrophys. J.* **215**, 733
Phillips, M.M., Baldwin, J.A., Atwood, B., Carswell, R.F.: 1983b, *Astrophys. J.* **274**, 558
Phillips, M.M., Taylor, K., Axon, D.J., Atherton, P.D., Hook, R.N.: 1984, *Nature* **310**, 554
Phillips, M.M., Turtle, A.J., Edmunds, M.G., Pagel, B.E.J.: 1983a, *Monthly Notices Roy. Astron. Soc.* **203**, 759
Pooley, G.G., Henbest, S.N.: 1974, *Monthly Notices Roy. Astron. Soc.* **169**, 477
Rafanelli, P., Bonoli, C.: 1984, *Astron. Astrophys.* **131**, 186
Richstone, D.O., Oke, J.B.: 1977, *Astrophys. J.* **213**, 8
Smith, R.M., Robertson, J.G.: 1985, *Monthly Notices Roy. Astron. Soc.* **212**, 809
Stockton, A.: 1976, *Astrophys. J. Letters* **205**, L113
Stockton, A.: 1982, *Astrophys. J.* **257**, 33
Stockton, A., MacKenty, J.W.: 1983, *Nature* **305**, 678
Stockton, A., MacKenty, J.W.: 1987, *Astrophys. J.* **316**, 584
Stockton, A., Wyckoff, S., Wehinger, P.A.: 1979, *Astrophys. J.* **231**, 673
Stone, R.P.S., Baldwin, J.A.: 1983, *Monthly Notices Roy. Astron. Soc.* **204**, 347
Tadhunter, C.N., Pérez, E., Fosbury, R.A.E.: 1986, *Monthly Notices Roy. Astron. Soc.* **219**, 555
van Breugel, W.J.M., Filippenko, A.V., Heckman, T.M., Miley, G.K.: 1985b, *Astrophys. J.* **293**, 83
van Breugel, W.J.M., Heckman, T.M., Butcher, H.R., Miley, G.K.: 1984b, *Astrophys. J.* **277**, 82
van Breugel, W.J.M., Heckman, T.M., Miley, G.K.: 1984a, *Astrophys. J.* **276**, 79
van Breugel, W.J.M., Miley, G.K., Heckman, T.M., Butcher, H.R., Bridle, A.: 1985a, *Astrophys. J.* **290**, 496
van Breugel, W.J.M., Heckman, T.M., Miley, G.K., Filippenko, A.V.: 1986, *Astrophys. J.* **311**, 58
van Heerde, G.M.: 1986, in *Proc. IAU Symp.* **119**, *Quasars*, eds. G. Swarup, V.K. Kapahi, p. 345
van Heerde, G.M.: 1988, *Astron. Astrophys.* (accepted)
Véron-Cetty, M.P., Véron, P.: 1985, ESO scientific report, No. 4 (VV)
Wampler, E.J., Robinson, L.B., Burbidge, E.M., Baldwin, J.A.: 1975, *Astrophys. J. Letters* **198**, L49
Wilson, A.S., Baldwin, J.A., Ulvestad, J.S.: 1985, *Astrophys. J.* **291**, 627
Wyckoff, S., Wehinger, P.A., Spinrad, H., Boksenberg, A.: 1980, *Astrophys. J.* **240**, 25